OUTLET GEOMETRICAL IMPACTS ON BLOWOFF EFFECTS WHEN USING VARIOUS SYNGAS MIXTURES IN SWIRLING FLOWS

Valera-Medina A
College of Physical Sciences and Engineering, Cardiff University, UK.

Vigueras-Zuniga MO
Mechanical Engineering, Universidad Veracruzana, Mexico.

Baej H
College of Physical Sciences and Engineering, Cardiff University, UK.

Syred N
College of Physical Sciences and Engineering, Cardiff University, UK.

Chong C T
UTM Centre for Low Carbon Transport in cooperation with Imperial College London, Universiti Teknologi Malaysia, Malaysia.

Bowen P.J.
College of Physical Sciences and Engineering, Cardiff University, UK.

Corresponding author contact: valeramedinaa1@cardiff.ac.uk, +44 (0) 2920-875948

ABSTRACT

Lean premixed swirl stabilized combustion is one of the most successful technologies for NOx reduction in gas turbines. The creation of inherent coherent structures such as recirculation zones is one of the main advantages of these flow-stabilised systems since these zones create regions of low velocity that allow heat transfer improvement between reactants and products while increasing residence time for unburned species. However, these effects can also affect the stability of the flame under lean conditions, with various instabilities that can appear during the combustion stage such as flashback, blowoff, autoignition, etc. These processes are even more complex when new alternative fuels are being used for power generation applications. Synthesis gases (syngas) are some of the most concerning out of the available range of fuels as their heating values, flame speeds, ignition energies, etc. are highly dependent on the combination of species that comprise them. Since new gas turbines need to deal with these new blends for fuel flexibility and current lean premixed swirled stabilized systems seem to be the most cost effective-technical option to keep NOx down, gas turbine designers need more information on how to properly design their equipment to achieve stable flames with low NOx whilst avoiding instabilities.

Therefore, this paper presents a study using numerical and experimental analyses to provide guidance on the use of CH_4/H_2/CO blends in tangential swirl burners. Methane content was decreased from 50% to 10% (volume) with the remaining amount being split equally between carbon monoxide and hydrogen. Ambient temperature conditions were assessed using a swirl number close to 1.0. Particle Image Velocity was used to experimentally validate numerical predictions and determine features of the coherent structures affecting the flame close to the nozzle. Modelling was carried out employing the k-ω SST turbulence model, providing more information about the impact of these structures and the flame turbulent nature close to blowoff limits. The study emphasizes the analysis of various nozzles with different angles and how these geometrical changes at the outlet of the swirl chamber affect the onset of blowoff. Recommendations on the use of RANS CFD modelling are provided on the basis of blend composition.

Keywords: Hydrogen, Carbon-monoxide, Syngas, Swirl, Blowoff.

INTRODUCTION

Fuel independence has been a major driver for the development of combustion systems during the last few decades, with the aim of finding technologies capable of achieving high fuel flexibility for

power generation. Swirl combustion has been widely used for this purpose as it provides high flame stability with relatively low emissions consequence of the creation of coherent structures such as the central recirculation zone (CRZ). The CRZ recirculates heat and active chemical species to the root of the flame, allowing flame stabilization in regions of relatively low velocity where the flow and the turbulent flame velocity are matched [1]. These flows can generate other vortical structures capable of producing benefits such as improved mixing, or cause detrimental effects by coupling with natural acoustic modes to give high levels of pressure fluctuation [2-5]. However, it has been recognised over the years that geometrical changes and the nature of the flow regime are critical parameters for the development, evolution and establishment of these structures, with studies and practical applications that demonstrate the changes in these regimes with slight variations of the system augmenting the complexity of the interactions that occur between flame and flow structures [5-9].

As new technologies develop, swirling flows are being deployed for the stabilization of more advanced fuels, amongst them Synthesis gas (syngas) products of gasification processes which contain highly hydrogenated blends with a combination of other species such as CO or CO_2. The use of syngas as a fuel source can potentially reduce CO_2, NOx and other pollutants [10] providing high flexibility in current gas turbines, especially those incorporated in systems known as Integrated Gasification Combined Cycles (IGCC) [11-12]. Therefore, the importance of the study of these fuel blends rests on the development of new gasification systems which employ biomass, waste or coal-based feedstock in order to reduce fossil fuel dependency while producing gaseous streams of enough calorific value to be used for power generation. Analyses of these new blends and their impact during the combustion process are crucial to designers working on this area, as many of these impacts are still unknown. Moreover, there is also a considerable need for validation studies that provide confidence on simulation tools, thus ensuring the most effective and less time-cost consuming methods are used for the design of these systems.

Previous studies [7, 13] have demonstrated that high hydrogen concentration considerably alters the combustion characteristics, thus changing the swirl number with its inherent effects on the size, shape and recirculated mass flowrate in the CRZ [7, 13]. The addition of CO_2 in the fuel blend can also lead to changes in viscosity, density and radiative heat transfer, thus changing the flow [13]. Experimental studies on emissions performance of syngas using different methods have been previously investigated by several researchers. Ge et al [14] investigated the combustion performance of non-premixed swirl syngas combustion, in particular the difference in emissions between H_2-lean and H_2-rich syngases with water dilution. Results showed that the level of NOx and CO emissions was constant for the range of syngases tested at low H_2O dilution. Joo et al [15] investigated H_2-rich combustion with enrichment of CH_4 using swirling partially premixed conditions, showing the reduction of NOx and flame temperature with the increase of CH_4. Zhang et al [16] conducted a study of syngas flames using a premixed opposed-jet flame. The key finding showed that CO_2 dilution has more profound effects on flame propagation and extinction rate than N_2.

Syngases keep capturing the attention of researchers; not only to achieve fuel flexibility but also to mitigate unwanted emissions. The volume ratio of H_2/CO in most syngas mixtures typically exceeds 0.25, where chemical kinetic and reaction mechanisms of hydrogen play a dominant role in syngas combustion. Hence, syngas generally exhibits large burning rates with small autoignition time [17]. Moreover, CO-rich syngases show different characteristic to H_2-rich blends. Low concentration of H atoms in the former affects fast oxidation pathways of CO, resulting in unstable combustion and high CO emissions that are not well understood [18]. Regarding hydrogen related phenomena, Azimov et al. [19] used biomass/coke derived syngas in a dual-fuel engine. The use of higher H_2 concentrations resulted in reduced CO and HC emissions but an increase in NOx, as temperatures in the combustion

chamber augmented. Similar trends of high NOx emissions for H_2-rich syngas were validated by Lee et al. [20] in a 60 kW industrial gas turbine using pure syngas without diluent. NOx emissions increased as the heat input increased. Higher CO was produced with lower combustion efficiency when the gas turbine was operated at low load. Nevertheless, Ouimette et al. [21] found different NOx trends under partially premixed combustion using similar syngases with H_2/CO ratios between 0.8 and 1.3. Watson et al. [22] also demonstrated that NO formation paths for syngases are mainly caused by thermal mechanisms, although N_2O and NNH routes have a considerable influence at lean equivalence ratios.

The variability in composition and heating value in different syngases represents a considerable challenge towards their use in practical combustion system, especially for systems that operate close to blowoff. Experiments conducted by Lieuwen et al [23] showed that small addition of hydrogen to methane blends can enhance the resistance to blowoff as a consequence of the high reactivity of H_2. Moreover, these fundamental studies demonstrated that the extinction strain rate of methane flames doubled with the addition of 10% (vol) H_2. Similarly, CO/CH_4 flames showed a variance in their extinction strain rate [23]. Strakey et al [24] studied the effects of hydrogen addition on flame extinction in a lean-premixed swirl-stabilized combustor operating on natural gas and air. They observed that increasing the hydrogen concentration in the fuel reduced the equivalence ratio before blowoff from 0.46 to 0.30. Schefer et al [25] conducted experiments on combustion characteristics of a premixed, swirl-stabilized flame to determine the effects of enriching methane with hydrogen under fuel-lean conditions. Hydrogen addition resulted in a significant change in the flame structure, indicated by a shorter and more robust flame. Li et. al. [26] studied the effects of diluents on blowoff trends using swirling premixed syngas flames. Results showed the impact of N_2 and the higher propensity of blowoff to occur at higher nitrogen ratios, with the inert gas dominating the behaviour of the flame at low hydrogen content. Sayad et al. [27] investigated the effect of swirl, showing that blowoff is significantly affected by these parameters. This was also documented by Garcia-Armingol and Ballester [28]. However, the studies have not shown any clear correlation between blowoff processes and the changes in geometrical parameters at the outlet of the swirl chamber;parameters that will affect the evolution of coherent structures in the combustion zone.

With some caveats noted by Shanbhogue et al [29], there is general agreement that the blowoff process is controlled by a competition between the fluid mechanical and chemical kinetic processes, which can subsequently be defined in terms of a Damköhler number. Current theories are based on a flamelet based description causing local extinction by excessive flame stretch [30-31]. However, limited work has been done on the impacts of other structures such as the Precessing Vortex Core (PVC) and its interaction with the flame to increase/decrease the propensity of blowoff effects. As it is well-documented, the structure can considerably increase the turbulence level close to the outlet of the nozzle, thus increasing stretch that can potentially initiate the propagation of blowoff [32-33].

Therefore, this paper presents experimental and numerical analyses to determine the impact of different nozzles when using various syngases on the propagation of the blowoff phenomena, linking the change in outlet geometry to the size and impact of recirculation zones, i.e. CRZ and PVC, to blowoff. Experimental results were obtained using Phase Locked PIV, while numerical calculations were done using the k-ω SST model with ANSYS Fluent. Recommendations and further work for the design of outlet nozzles based on the hydrogen content of the syngas blend are provided at the end of the study. The novelty of the study is found on the effect of the nozzle on blowoff trends with recommendations to use RANS CFD modelling only with certain fuel blends.

SETUP

A generic swirl burner constructed from stainless steel was used to perform the experimental trials at atmospheric conditions (1bar, 293K). A schematic of the generic burner is presented in Figure 1. A

single tangential inlet (a) feeds the premixed air and fuel to a swirl chamber (c). Gas is distributed to a tangential swirler (d). Swirling unburned reactants then reach the main combustion zone via a steel sleeve (e) before combustion takes place. A central diffusion fuel injector (not used in these tests) extends centrally through the combustor body (b). Air and fuel were fed using OMEGA variable area flow meters, and Coriolis meters were used to determine the flowrates with 0.5% accuracy.

A geometrical Swirl number (S_g) of 1.05 was used. Different nozzle chamfers, α, of 30°, 45°, and 60° were employed, Figure 2. Wall thickness was kept constant to ensure that swirl at the outlet would be the same. Unconfined and confined conditions were assessed. Confinement was attained via a quartz tube with an area expansion ratio of 8.47, and burner nozzles with internal diameters of D = 0.028 m. An L/D ratio, L being the nozzle length, was kept at 1.00 for all the nozzles.

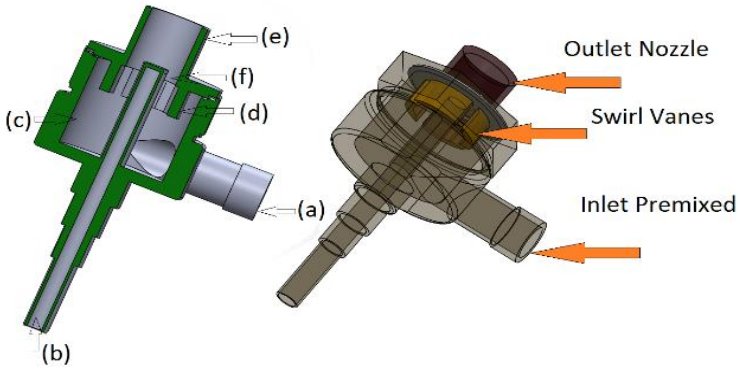

Figure 1. Schematic of the generic burner

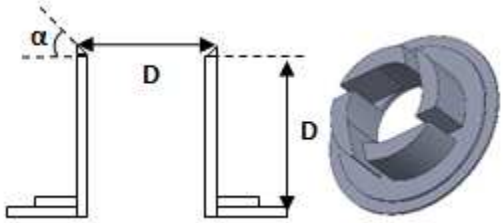

Figure 2. Angular nozzle and geometrical swirl respectively.

Experiments were conducted using a range of CH_4, H_2 and CO blends, Table 1. First experiments were run at different equivalence ratios to determine stability trends. Then, experiments were carried out at the same power output, Table 2, to correlate the impact of blend compositions using numerical and experimental analyses. These flowrates allowed Re between 10,900 to 14,000 (i.e. based on the outlet diameter, D). Further experiments were performed using Low Power (LP = 2.50 kW), Medium Power (MP = 6.45 kW) and High Power (HP = 10.45 kW) conditions to determine any relation between nozzles, gases and power loads.

Table 1. Gas compositions

Gas number	Gas compositions	LHV [MJ/kg]
Syngas 1	10% CH_4 + 45%H_2 + 45%CO	63.53
Syngas 2	20% CH_4 + 40%H_2 + 40%CO	62.08
Syngas 3	30% CH_4 + 35%H_2 + 35%CO	60.52
Syngas 4	50% CH_4 + 25%H_2 + 25%CO	57.51

Table 2. Experimental and CFD conditions, 6.45 kW.

Gas No	Ṁ fuel [g/s]	Ṁ Air [g/s]	α°	Total [g/s]	Φ
Syn1	0.101	1.41	30°	1.51	0.425
Syn1	0.101	1.40	45°	1.50	0.428
Syn1	0.101	1.38	60°	1.48	0.453

Syn2	0.104	1.55	30°	1.66	0.485
Syn2	0.104	1.55	45°	1.65	0.486
Syn2	0.104	1.48	60°	1.59	0.508
Syn3	0.107	1.63	30°	1.73	0.563
Syn3	0.107	1.67	45°	1.78	0.548
Syn3	0.107	1.65	60°	1.75	0.557
Syn4	0.113	1.83	30°	1.95	0.689
Syn4	0.113	1.79	45°	1.90	0.707
Syn4	0.113	1.83	60°	1.94	0.692

EXPERIMENTAL TECHNIQUE

A Phase Locked Particle Image Velocimetry system was employed to characterize the flow field experimentally, Figure 3. Strong Precessing Vortex Cores (PVC), Figures 4 and 5, and associated structures were found. Their frequencies were characterised via a PCB Piezotronics 378B02 condenser microphone located 0.01 m upstream from the burner outlet which tracked the frequency changes of the High Momentum Flow Region (HMFR) formed by the precessing shearing flow. The microphone condenser signal was redirected to a signal conditioner with low and high band pass to recognise frequencies above 10 Hz and up to 2,500 Hz. The reconditioned signals were redirected to trigger a BNC Model 500 Pulse Generator, whose TTL signal was sent to a Dantec Stereo PIV system for triggering purposes. The PIV system consists of a dual cavity Nd: YAG Litron Laser of 532 nm capable of operating at 5 Hz. A 1mm thick sheet was produced using Dantec Dynamics laser sheet optics (9080X0651). A Hi Sense MkII Camera model C8484-52-05CP was employed in combination with a 60mm Nikon lense, allowing a field of view of ~75x75 mm with a resolution of 5.35 pixels per mm and a depth of view of 1.5 mm.

Calibration was performed using a physical grid provided by the manufacturer. The inlet air was seeded with aluminum oxide by a seeder positioned 1.0m upstream of the burner inlet. A frame-to-frame adaptive correlation technique was employed for post-processing the data, using a minimum interrogation area of 32x32 pixels and a maximum of 64x64. 500 pairs of frames were used to create average velocity maps.

Results are reported in terms of Inlet Tangential Velocity at which the premixed reactants ingress into the swirl chamber. This value has previously proved a good correlation between the flow behaviour and the onset of various structures and instabilities [34].

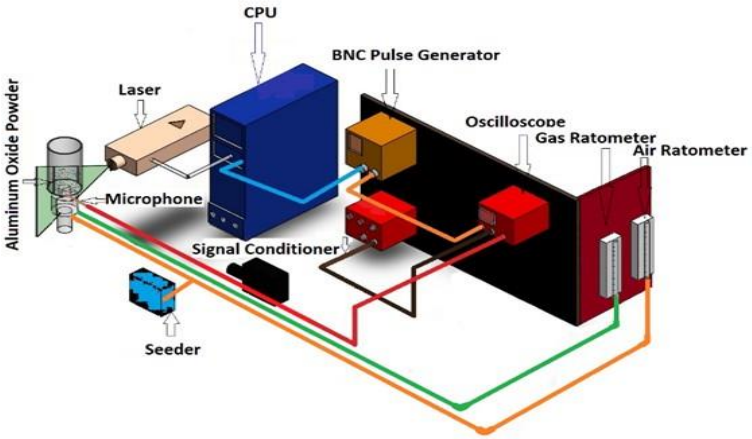

Figure 3. Schematic setup of the entire system. Axial-radial and radial-tangential planes were obtained.

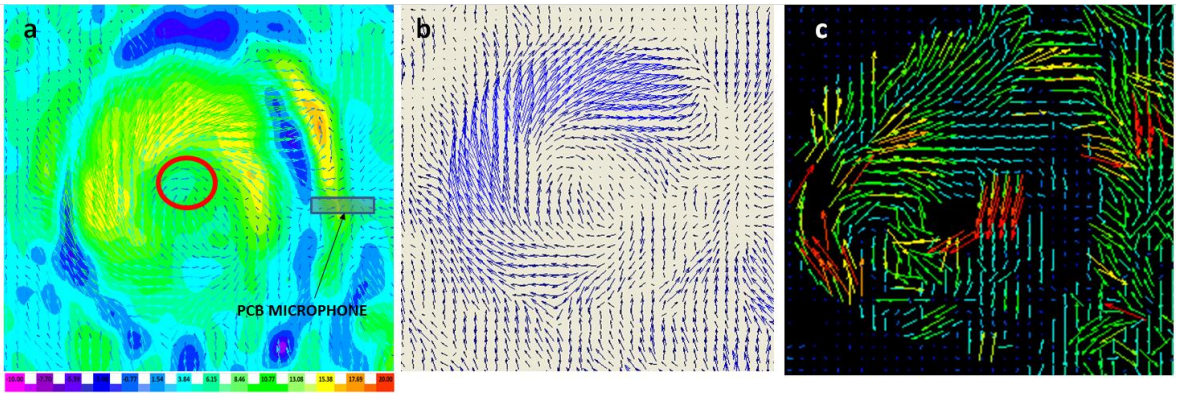

Figure 4. Flow characteristics exactly at the outlet of the burner a) Radial-tangential velocity contours; b) Phase-averaged vectors; c) Instantaneous velocity vectors. Re~14,000 and α=45°. PVC (red) encircled. Velocity in [m/s].

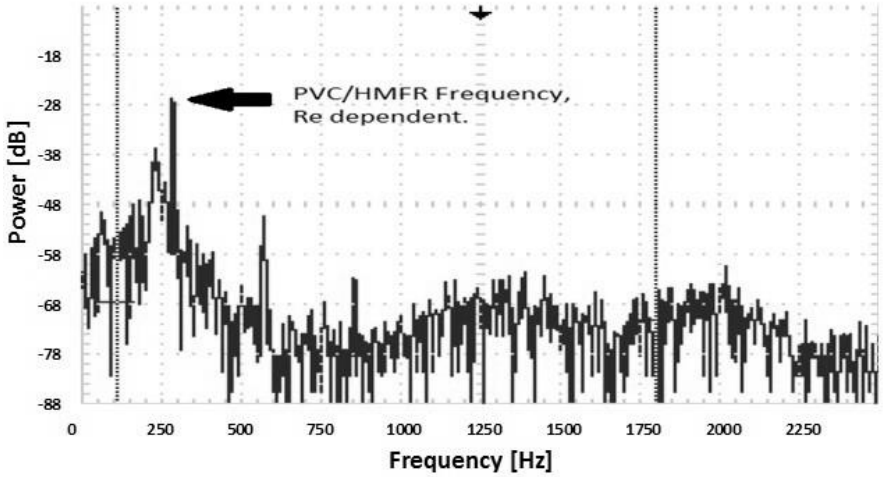

Figure 5. Fast Fourier Transform frequency analysis at ~10,900 Re. PVC/HMFR peak depends on Re.

NUMERICAL TECHNIQUE

Inlet conditions were set at 1 bar and 300 K. Various solvers were investigated with preliminary tests being run with pure methane at flowrates between 1.51 and 1.94 g/s. After an experimental comparison was carried out, it was concluded that the best agreement was observed using the κ-ω SST model [35]. To obtain the specific dissipation rate ω, and turbulence kinetic energy k, the following transport equations are applied:

$$\frac{\partial}{\partial t}(\rho k) + \frac{\partial}{\partial x_i}(\rho k u_i) = \frac{\partial}{\partial x_i}\left(\Gamma_k \frac{\partial k}{\partial x_j}\right) + G_k - Y_k + S_k \quad (1)$$

and

$$\frac{\partial}{\partial t}(\rho \omega) + \frac{\partial}{\partial x_i}(\rho \omega u_i) = \frac{\partial}{\partial x_i}\left(\Gamma_\omega \frac{\partial \omega}{\partial x_j}\right) + G_\omega - Y_\omega + D_\omega + S_\omega \quad (2)$$

G_k represents the generation of turbulence kinetic energy due to mean velocity gradients. G_w represents the generation of ω. Γ_k and Γ_ω represent the effective diffusivity of k and ω, respectively. Y_k and Y_ω represent the dissipation of k and ω due to turbulence. D_ω represents the cross-diffusion term. S_k and S_ω are user-defined source terms [36].

Simulations were performed using all syngases in Table 2 under fully premixed conditions with ANSYS FLUENT 14.5. The pre-processor used to construct the model grid was ICEM 14.5.7. Three meshes

were examined in order to perform a mesh independency analysis, Table 3. After carrying out the analyses, it was decided to use a medium size mesh that consists of ~796,878 nodes and 796,878 elements, and that provided mesh-independent results when compared to the high size mesh. The mesh was designed with a structured grid creating a higher node density in areas where the flow was expected to change considerably, i.e. close to the nozzle, Figure 6. A Courant number <0.55 was obtained for this particular mesh. The PRESTO discretization scheme was used for pressure, with the SIMPLE scheme for pressure-velocity coupling using a convergence criterion set at 10^{-4}. Non-slip wall boundary conditions were defined using adiabatic conditions at 1 bar inlet pressure and inlet temperatures of 300K for a Steady-state analysis.

Table 3. Various mesh densities for independency analysis.

Mesh Density	Number of Elements
High	2,275,788
Medium	796,878
Low	289,124

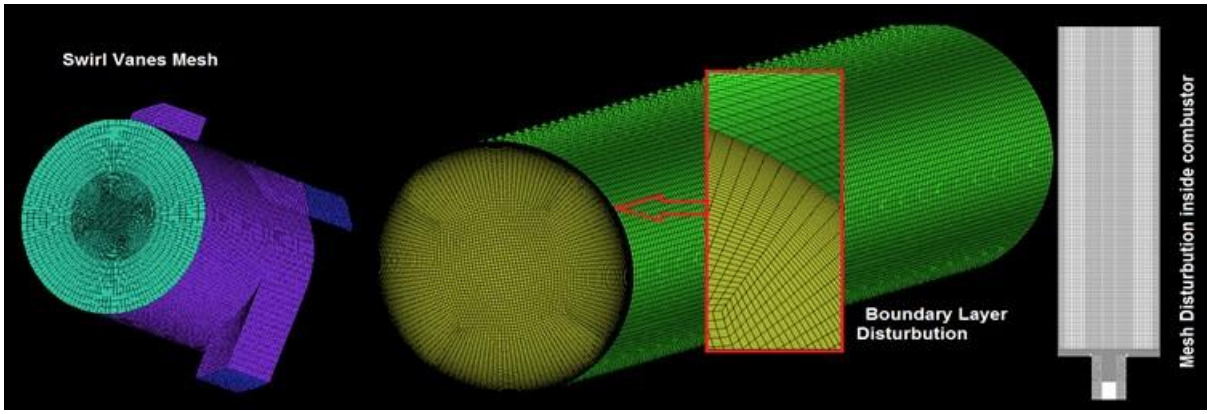

Figure 6. Mesh Distribution and boundary layer.

Results and Discussion

Figure 7 shows a comparison of Lean BlowOff (LBO) limits obtained using different syngases and various nozzles. There is a clear effect in terms of the increase of blowoff resistance at higher hydrogen concentrations, with Syngas-1 being the blend with less susceptibility to this instability and a larger operability range. This was expected as documented elsewhere [24]. However, a less expected trend was the change in behaviour caused by the nozzle angle. It can be seen that some data follow linear trends, especially with the experiments using the 45˚nozzle and Syngas-1. As hydrogen is decreased, the trend becomes less linear, with Syngas-4 showing measurements far from the main trend line. Moreover, as the angle is decreased/increased from the 45˚ case, the results become more chaotic, implying a breakdown in the controlling phenomena due to a process linked to the propagation of non-linear phenomena.

From the results, it is clear that Syngas-1 shows a similar trend under all unconfined conditions. Furthermore, there is a similar behaviour for the confined cases using Syngas-1, with the same LBO equivalence ratios at the same tangential velocities. Conversely, the increase in methane has completely shifted the blowoff limits using different geometries, especially under unconfined conditions, Figure 7. Since the Damköhler number is the same for these cases, it is clear that another phenomenon exists close to the nozzle that affects the blowoff propagation.

It has been theorised that the phenomenon is caused by the change in shape of the CRZ, which in conjunction with the shearing flow, feeds another structure named the Precessing Vortex Breakdown (PVC) [32]. The strength and turbulence generated by this PVC will depend on the shape of the CRZ and its contact with the shearing flow. Therefore, changes in the geometrical conditions of the system will alter the PVC and its impacts on the flow. However, results suggest that although the structure will change using different nozzles, their impact will be negligible using more reactive fuels such as highly hydrogenated blends. As the hydrogen content is reduced, the impact of this (and other structures) will be greater on the flame, consequently leading to earlier blowoff.

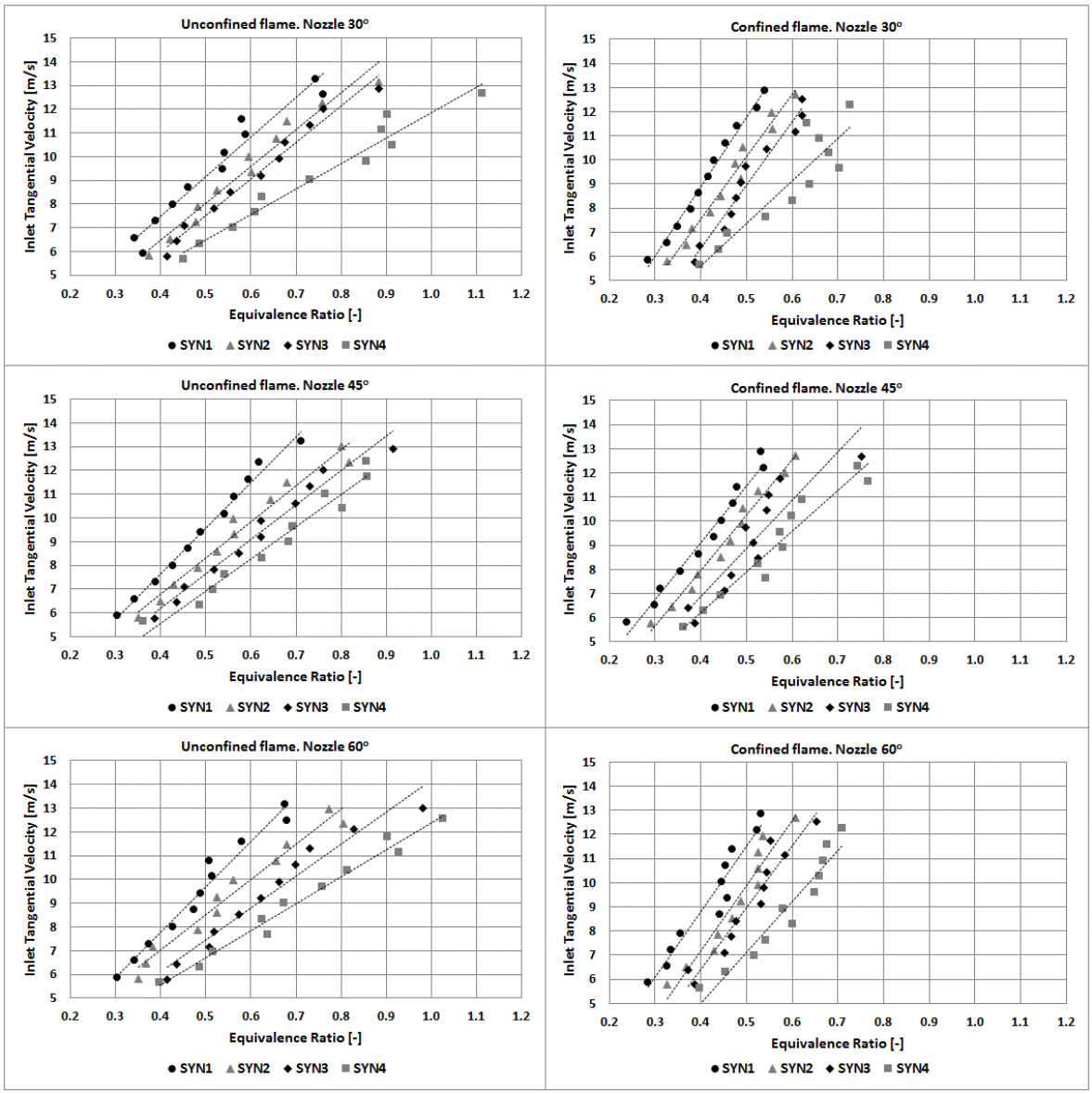

Figure 7. Comparison of blowoff limits using unconfined and confined conditions with various syngases and nozzle geometries.

Further tests were carried out using the same blends but with 3 different power outputs. The LBO limits for all cases, Figure 8, show the effects of the nozzle angle using all blends with a special emphasis on the changes produced when using Syngas-4. It is believed that the shift in LBO limits between cases at low hydrogen concentration is a consequence of the interaction of the CRZ-PVC with the flame. This interaction has been previously studied elsewhere [2, 32], showing a considerable increase in turbulence where both structures collide.

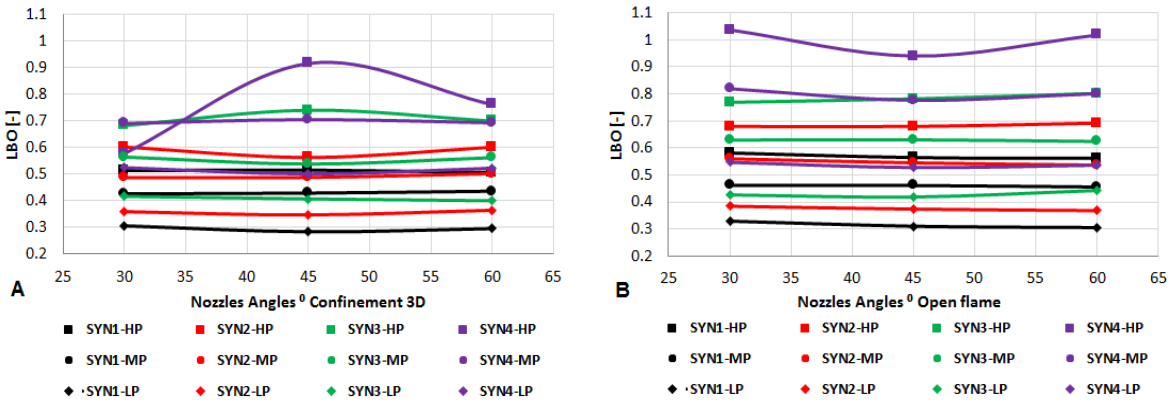

Figure 8. Comparison of the effect of outlet nozzle angle on LBO equivalence ratio for all syngases at LP, MP and LP. Trends are added to visualize the change. A) Unconfined case; B) Confined conditions.

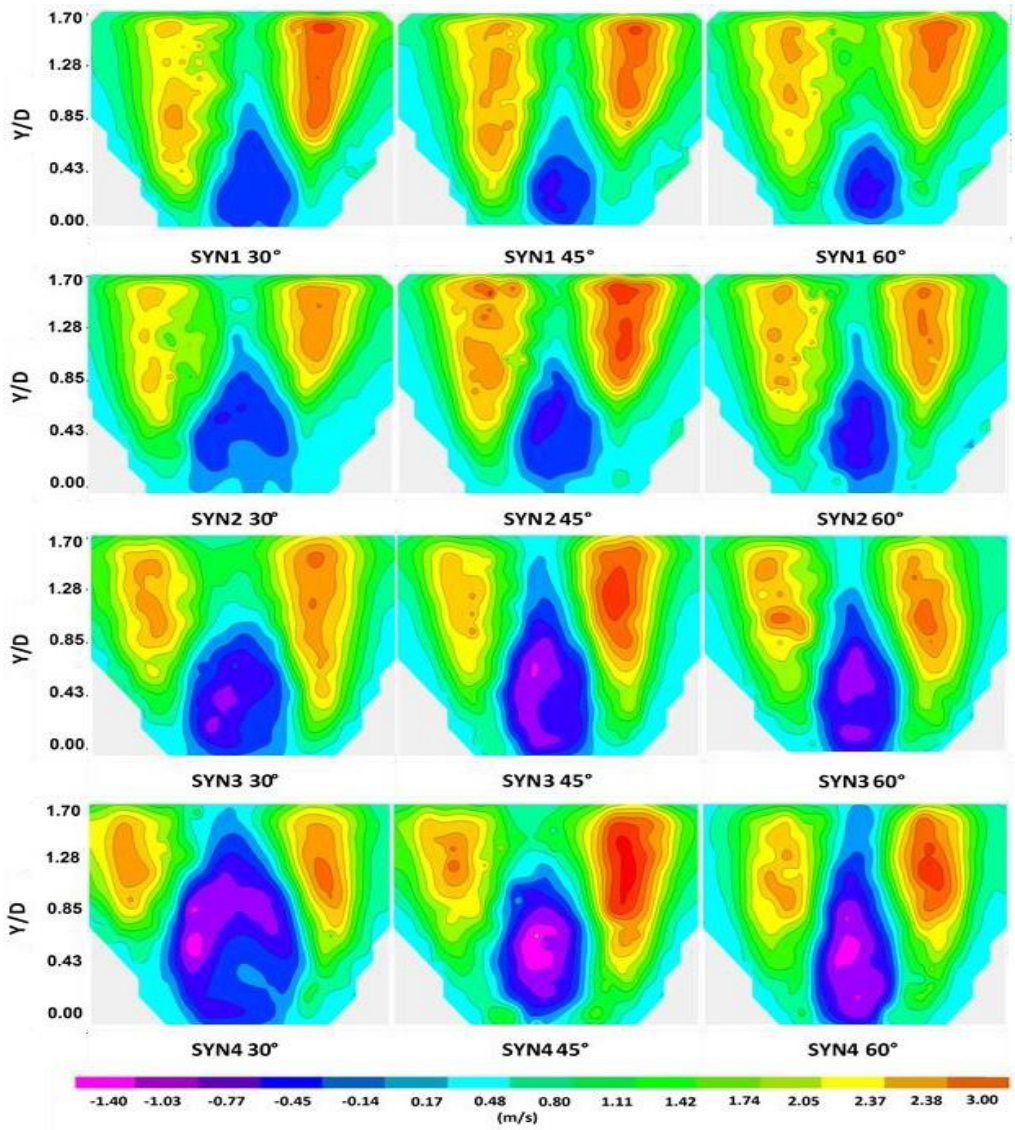

Figure 9. Experimental PIV CRZ boundary contours for each blend and nozzle angle. Axial velocity. Units in [m/s].

PIV velocity contours were obtained to determine the changes of the CRZ using all different blends and nozzles under unconfined conditions, Figure 9. The CRZ boundaries were defined in a velocity range of -1.40 to 0.170 m/s, with a streamline post-processing showing the existence of the recirculation zone, Figure 10.

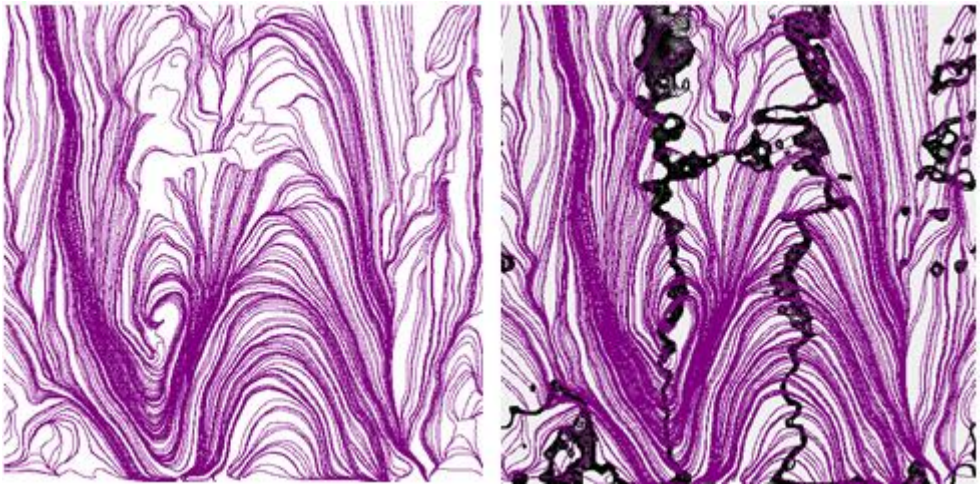

Figure 10. Left) Streamlines showing the presence of recirculation across the flow. Right) Negative velocity regions in the flow showing the boundaries of the CRZ.

It is clear that the CRZ distortion occurs for all cases in Table 1 using the three nozzles. Therefore, a change in the interaction between PVC and CRZ would be expected. As follows, this interaction is theorised as a consequence of the lack of visual access to the outlet of the nozzle, a problem related to the high reflection of the laser at this position.

The use of more hydrogen, i.e. Syngas-1, shows how the faster reactivity of the molecule shortens the CRZ with a slight change in the features of the structure. On the other hand, the reduction of hydrogen creates a wider variety of CRZs, with the most notorious case being Syngas-4. For instance, the use of a 30˚ nozzle shows wider structures. Therefore, a bigger CRZ would be expected to have less contact with the flame through its entire profile, i.e. with the flame only being in contact with the bottom of the CRZ. As the nozzle angle is increased to 45˚, the redirection of the shearing flow reduces the size of the CRZ but increases the interaction between the CRZ-PVC simultaneously. Further increase of the angle to 60˚ reduces, even more, the width of the structure, pushing the CRZ and the shearing flow closer to increase turbulence and the impacts of the PVC towards the flame, augmenting the propensity of blowoff. This is confirmed from the unconfined flame trends, Figure 7.

It is also noticeable from the results that for the use of Syngas-4 under confinement the best option would be to use a nozzle with an angle of 60˚. Compared to the other geometries, this nozzle shows measurements that are more stable and closer to the trend line. It is known that under confined conditions, outside air neither flushes the flame nor reduces its temperature. As previously stated, the 60˚ case should produce a stronger CRZ-PVC interaction with the likelihood of greater stretching caused by the shearing flow. However, since the flame is confined and well preserved, this greater stretching and structural interaction seem to enhance the flame, likely a consequence of the better distribution of species caused by the PVC and flame elongation. This was a concept previously proposed by O'Doherty et al. [37-38].

Figure 11 shows a merge of both PIV velocity maps and u'-v' turbulence intensity. The purpose of these contours was to provide an estimate of the percentage of turbulence outside the CRZ. Although it is recognised that total turbulence cannot be obtained through this methodology since w' cannot

be resolved, it was acknowledged that some insights of the turbulence parameters could be depicted via 2D PIV, thus being of indicative nature for correlation with CFD.

It is clear that the location of the CRZ defines the boundaries where turbulence increases, another indication of the interaction between flow and structures. There is a considerable contrast of the shape and size of the CRZ when using the four syngases and the three different nozzles. The maps revealed the increase in turbulence intensity surrounding the CRZ opposite to the position of the microphone (PVC), Figure 11. This phenomenon is related to the interaction between the low momentum flow and its interaction with the CRZ. On the other hand, the highest peak of turbulence is located where the PVC is measured, appearing at the bottom, a region that has been previously defined where the PVC-CRZ collide at their highest strength [27], thus suggesting a clash that stirs up the flow field.

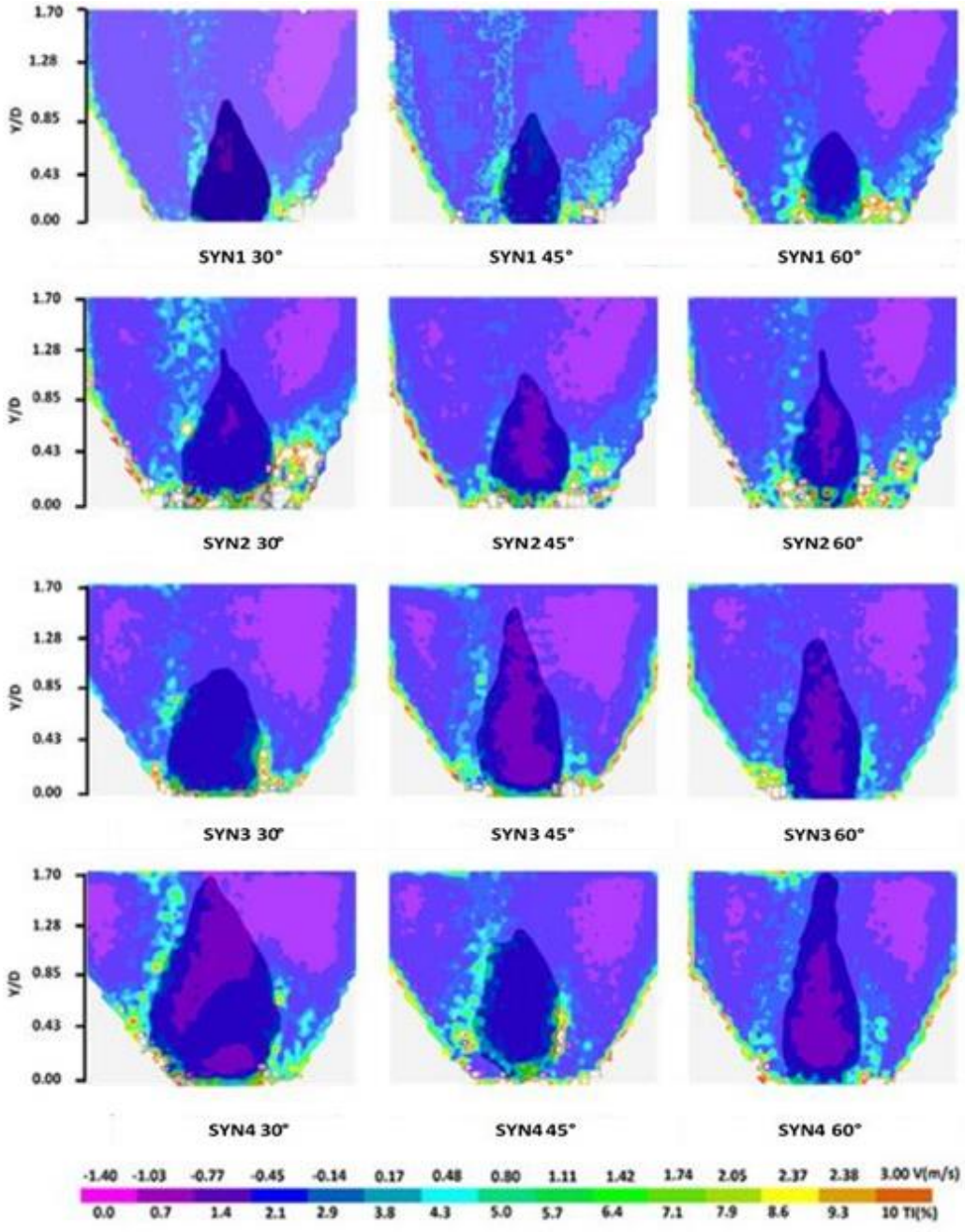

Figure 11. Turbulent intensity matched with CRZ boundary (shaded) using a scale of turbulent intensity of 0-10% and axial velocity ranging from -1.40 to 0.170 m/s.

Analyses were performed using the PIV results, Figure 12. The progressive reduction of hydrogen increases the strength of the recirculation zone, whilst reducing the velocity of the shearing flow. This is also observed from the point at which the curves cross the abscissas axis, indicating that the CRZ reduces its width whilst the shearing flow is getting stronger with a hydrogen increase, as expected. Radial velocities are also affected as a consequence of the increase of reactivity, Figure 13. This also affects the relationship between shearing flows and formation of the CRZ.

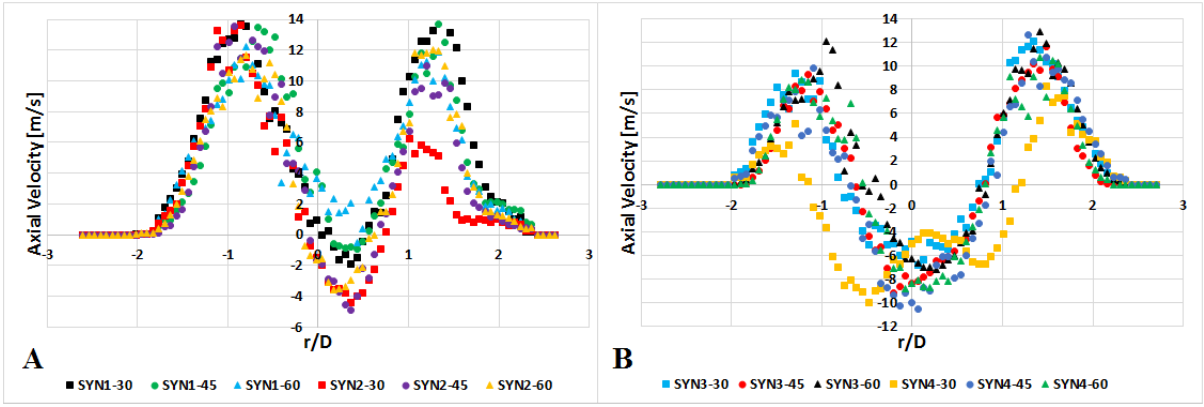

Figure 12. Axial velocity at y/D 0.107. A) Syngases 1 and 2; B) Syngases 3 and 4.

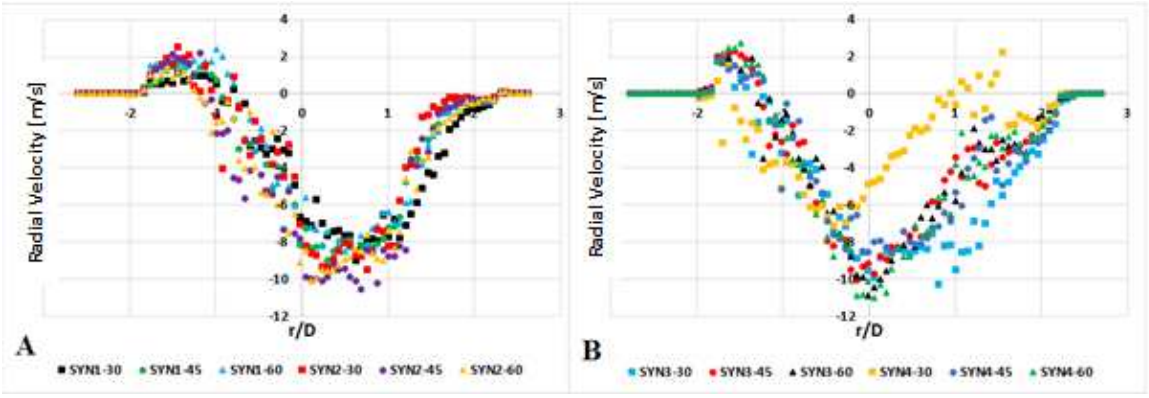

Figure 13. Radial velocity at y/D = 0.107. A) Syngases 1 and 2; B) Syngases 3 and 4.

Experimental results have demonstrated that the shape and strength of the CRZ can drastically change depending on the alterations imposed in both fuel composition and flow. CFD analyses using the SST-k-ω model were carried out to observe the change in the size of the CRZ under confinement. Simulations were calibrated by using pure methane, Figure 14. It is recognized that the CFD under-predicts the location of the shearing flow. However, further comparison between experimental results and CFD predictions for the CRZ size demonstrate that good correlation was achieved between both techniques. A standard deviation of ~0.51m/s was observed opposite to the measuring point and central area, with a spike of ~3.96m/s next to the microphone. This shows consistency with previous test performed somewhere else [32], with the region close to the PVC producing the greatest deviations.

However, the correlation between experiments and simulations is only clear when comparing the size of the CRZ, negative and positive velocities, which show relative errors of 3.07%, 3.06% and 4.12%, respectively. When comparing the results of the regions outside of the shearing flow there is no correlation, with a staggering 530.16% difference between experiments and numerical results.

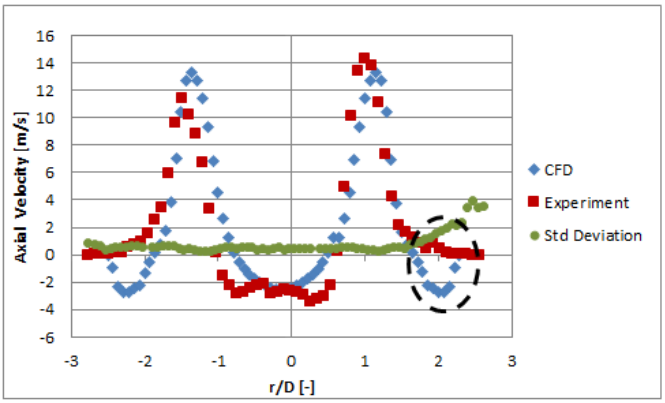

Figure 14. Correlation between CFD and experimental simulations using pure methane. 0.107D from nozzle outlet. The experimental standard deviation was relatively constant, at ~0.5m/s. However, there is poor correlation outside of the shearing flow (encircled region).

Results are presented in Figure 15 and Table 5. It is evident that there is no significant difference between experimental results and CFD calculations in most cases. Worst predictions were obtained using the 30˚ nozzle and the slowest Syngas-4, and the 60˚ nozzle with the fastest Syngas-1. This lack of accuracy seems to be linked to 3-Dimensional large structures such as the PVC that are not accurately predicted by this model and the lack of resolution for fast reaction phenomena, respectively.

Therefore, predictions using confinement were carried out to simulate more representative conditions to those used in industry. Table 6 shows numerical results with confinement, illustrating length and width of the CRZ with each gas and all nozzles. The effect of confinement has an extremely important effect upon the CRZ, thus its interaction with the PVC. As discussed by Syred [1] confinement can dramatically alter the size and shape of the CRZ and external recirculation zones formed as the swirl burner flow expands. Figure 16 shows the numerical results for the CRZ, which denote the change in length and diameter of the structure. It is clear that acute elongation is produced by the confinement, likely a consequence of lower pressure decay. It was found that the angle of 60° produces larger CRZs with the narrowest profiles, as expected.

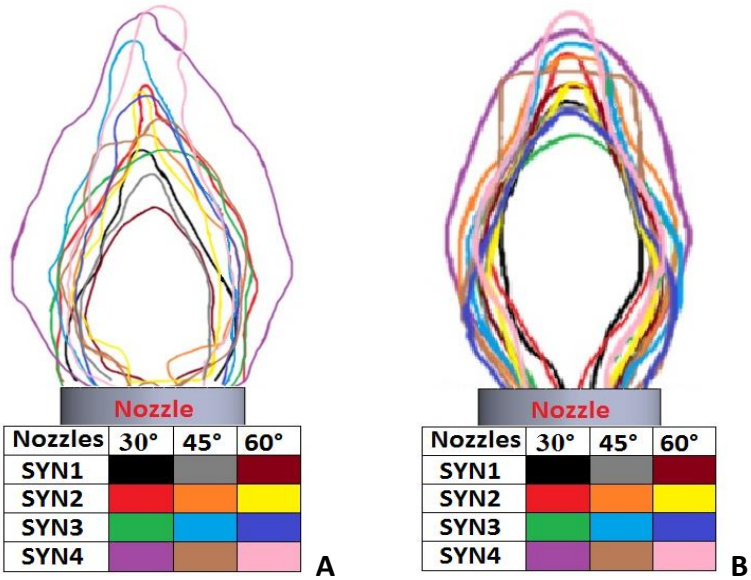

Figure 15. (A) Experimental and (B) CFD simulations for CRZ, respectively.

Table 5. Experiments, numerical simulations and difference [%] between both studies. Greatest discrepancies highlighted.

Gas	30°		45°		60°	
Experimental						
	Width	length	Width	length	Width	length
SYN1	1.35D	1.92D	0.97D	1.73D	1.01D	1.43D
SYN2	1.50D	2.44D	1.28D	2.07D	1.13D	2.41D
SYN3	1.54D	1.95D	1.43D	2.86D	1.24D	2.41D
SYN4	2.11D	3.12D	1.43D	2.22D	1.24D	3.16D
Numerical						
SYN1	1.33D	2.00D	0.90D	1.94D	1.13D	1.80D
SYN2	1.47D	2.34D	1.27D	2.07D	1.20D	2.41D
SYN3	1.33D	1.74D	1.33D	2.67D	1.13D	2.41D
SYN4	1.60D	2.67D	1.34D	2.27D	1.14D	2.63D
Difference between Experimental and Model [%]						
SYN1	1.48	4.17	7.20	12.1	11.80	25.8
SYN2	2.00	4.09	0.78	0.00	6.19	0.00
SYN3	13.60	10.70	6.90	6.60	8.87	0.00
SYN4	24.00	14.00	6.20	2.20	8.00	16.00

Table 6.Numerical simulations under confinement.

	30°		45°		60°	
	Width	length	Width	length	Width	length
SYN1	1.85D	4.70D	1.90D	4.30D	1.40D	9.60D
SYN2	1.80D	5.20D	1.85D	4.60D	1.80D	4.70D
SYN3	1.90D	5.40D	1.90D	7.20D	1.80D	5.20D
SYN4	1.90D	5.80D	1.90D	4.60D	1.70D	4.00D

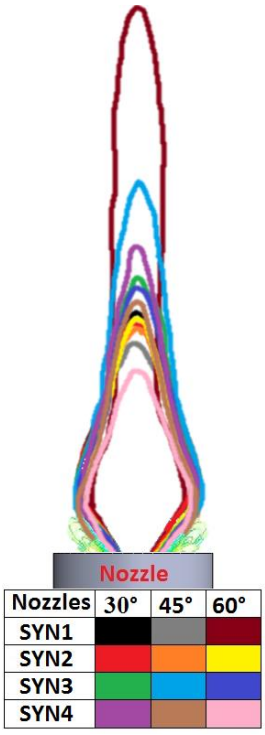

Figure 16. CFD results of CRZ contours of all blends and nozzles using confinement.

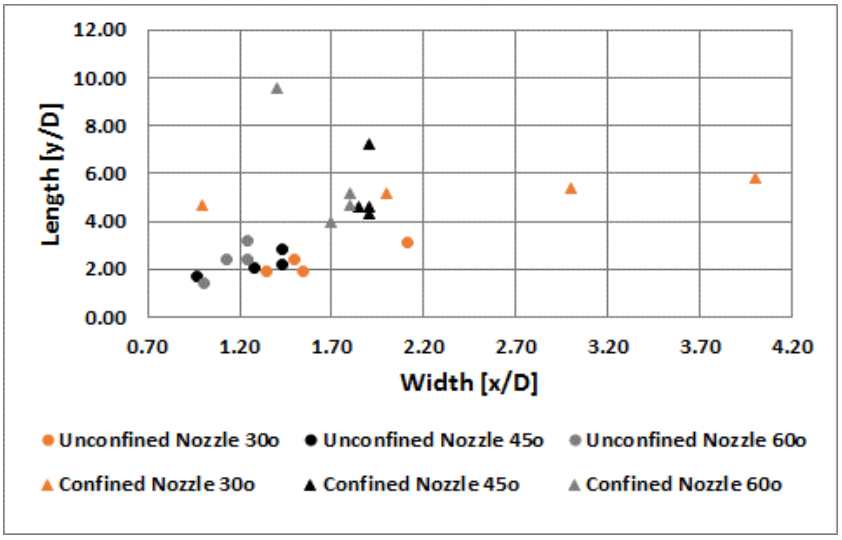

Figure 17. CFD comparison of CRZ between unconfined and confined cases.

Furthermore, a comparison between cases, Figure 17, shows that most of the CRZs using confined conditions and 45˚- 60˚ nozzles have similar features. This could be another reason for the better behaviour of these nozzle using these alternative fuels, as observed in figure 7.

Final results were obtained using CFD to account for the chemical time scale in 3-D swirling flows. Increasing the mole fraction of hydrogen in the mixture produces faster chemical reactions, Figure 18, and shorter turbulent time scales due to the higher thermal diffusivity of hydrogen and laminar flame speed, as expected. However, two interesting phenomena occur using a) Syngas-3 and nozzle 45˚, and b) Syngas-4 with a 30˚ nozzle, respectively. For the first case, the lowest chemical time scale is produced using 35% CO and an angle with moderate shear. This simulation showed a good experimental-numerical correlation, Table 5. Although Syngas-3 has a large concentration of hydrogen, the high CO content seems to be slowing down the reaction to a point of allowing the enlargement of the CRZ. Although the impacts of the PVC to this configuration would be considerable with the 45˚ angled nozzle, the high reactivity would also limit the response of the flame to the CRZ-PVC interaction, as previously stated. Therefore, these assertions lead to a Da phenomenon, where H_2 is inhibited by CO and CH_4. Thus, it is at this point of 35% CO that the injection of the latter can control the reaction speed when using 35% H_2 while avoiding the detrimental effects of the CRZ-PVC interaction. On the other hand, the case with Syngas-4 using a 30˚ nozzle has been previously depicted as a condition where the CRZ-PVC interaction would invoke its highest impacts. However, as observed in Table 5, assertions for this blend would need to be correlated with more advanced models.

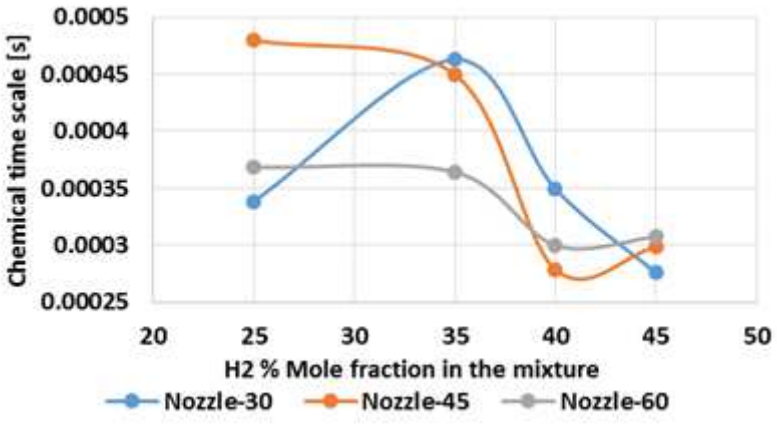

Figure 18. Chemical time scale vs the percentage of hydrogen in the mixture.

Recommendations

These results suggest the use of a greater nozzle angle, i.e. 60˚, under confined, industrially relevant conditions when using a low hydrogen concentration blend in order to promote the elongation of the flame and greater interaction between species and CRZ-PVC. If highly hydrogenated blends are going to be used, a 30˚ nozzle angle should be used in order to reduce impingement to the nozzle walls, as the nozzle angle will have small effects on the blowoff propensity. Finally, with a concentration of 35% or lower, hydrogen is slowed down considerably using a similar concentration of CO in a methane-based blend, thus hydrogen concentrations need to be above this limit to ensure greater blowoff resistance, likely as a consequence of negligible effect product of the PVC-CRZ interaction.

RANS SST k-ω simulations do not provide good correlation for conditions with high shearing stretch and high reactivity (i.e. α=60˚ and high H_2), and low reactivity with low shearing stretch (i.e. α=30˚ and low H_2), as the model does not depict the high reactivity of the flame while missing the adequate resolution of structures such as the Precessing Vortex Core. Thus, the model is recommended for design purposes as long as blends and flow conditions are different to those previously mentioned.

It is also recommended that further studies using LDA are conducted to demonstrate the interaction between structures at the outlet, avoiding the high reflection that PIV produces close to the burner outlet. This will provide further experimental details of the PVC-CRZ interaction.

Conclusions

Experiments and numerical simulations were conducted in a premixed swirl burner under unconfined and confined conditions to determine the impacts of outlet geometrical constraints using various syngas mixtures on the propensity of blowoff. The conclusions obtained are:

- The use of highly hydrogenated blends does not show any critical difference between cases, and blowoff is very similar between conditions, demonstrating that blowoff is not affected by any geometrical change at the outlet using these blends.
- The use of blends with low hydrogen concentration show considerable change in their blowoff behaviour under unconfined conditions as a consequence of the interaction of structures with the flame that is not only being affected by these structures but also by air entrainment from the surroundings, thus showing low resistance to the instability through the effects of the CRZ-PVC interaction.
- Confinement avoids air entrainment from the surroundings, thus reducing flame heat losses. As a consequence, the flame can withstand the CRZ-PVC interaction, which improves the stability of the flame as a consequence of better mixing and greater elongation.
- CFD results show that a 30˚ nozzle angle will produce considerably wider flames, while the 45˚ and 60˚ geometries will produce CRZs of similar sizes.
- It is recommended that under confined conditions a 60˚ nozzle is used to promote better flame and more stable blowoff conditions. Similarly, if highly hydrogenated blends are going to be used, a 30˚ nozzle angle should be used to reduce impingement to the nozzle walls, as the nozzle angle will have small effects on the blowoff propagation.
- A 35% or lower hydrogen content blend with the same amount of carbon monoxide in a methane-based blend seems to produce slower reactions, thus increasing the propensity of blowoff. Thus, hydrogen needs to be kept higher than this value to ensure greater blowoff resistance under swirling conditions.
- RANS SST k-ω can be used for conditions that do not present excessive shearing stretch or high reactivity.

Acknowledgements

The authors gratefully acknowledge the support of the Welsh Government and the European Union through the program FLEXIS West, project number 511378.

References

[1] Syred N, 2006. A review of oscillation mechanisms and the role of the PVC in swirl combustion systems, *Prog Energy Combust Sci* 32 (2): 93-161.

[2] Valera-Medina A, Syred N, Bowen P, 2013. Central Recirculation Zone Analysis using a Confined Swirl Burner for Terrestrial Energy, *J AIAA Propulsion Power* 29(1): 195-204

[3] Shtork S, Viera N, Fernandes E, 2008. On the Identification of helical instabilities in a reacting swirling flow, *Fuel* 87: 2314-2321.

[4] Valera-Medina A, 2009. Coherent Structures and their effects on Processes occurring in Swirl combustors, PhD Thesis, Cardiff University, Wales, U.K.

[5] Vigueras-Zuñiga MO, Valera-Medina A, Syred N, 2012. Studies of the Precessing Vortex Core in Swirling Flows, *J App Res Tech* 10: 755-765.

[6] Hwang J, Bouvet N, Sohn K, Yoon Y, 2013. Stability characteristics of non-premixed turbulent jet flames of hydrogen and syngas blends with coaxial air, *Int J Hydrogen Energy* 38(12), pp. 5139–5149.

[7] Ballachey GE, Johnson MR, 2013. Prediction of blowoff in a fully controllable low-swirl burner burning alternative fuels: Effects of burner geometry, swirl, and fuel composition, *Proc Combust Inst* 34(2): 3193–3201.

[8] Ranga Dinesh KKJ, Luo KH, Kirkpatrick MP, Malalasekera W, 2013. Burning syngas in a high swirl burner: Effects of fuel composition, *Int J Hydrogen Energy* 38(21): 9028–9042.

[9] Valera-Medina A, Syred N, Bowen P, 2013. Central recirculation zone visualization in confined swirl combustors for terrestrial energy, *J AIAA Prop Power* 29 (1): 195-204.

[10] Burbano HJ, Pareja J, and Amell AA, 2011. Laminar burning velocities and flame stability analysis of H2/CO/air mixtures with dilution of N2 and CO2, *Int J Hydrogen Energy* 36(4): 3232-42.

[11] Fu J, Tang C, Jin W, Thi LD, Huang Z, and Zhang Y, 2013. Study on laminar flame speed and flame structure of syngas with varied compositions using OH-PLIF and spectrograph, *Int J Hydrogen Energy* 38(3): 1636-43.

[12] He F, Li Z, Liu P, Ma L, and Pistikopoulos EN, 2012. Operation window and part-load performance study of a syngas fired gas turbine, *Appl Energy* 89(1): 133-41.

[13] Lewis J, Valera-Medina A, Marsh R, Morris S, 2014. Augmenting the structures in a swirling flame via diffusive injection, *J Combust* 2014: ID 280501.

[14] Ge B, Tian Y, Zang S, 2016. The effects of humidity on combustion characteristics of a nonpremixed syngas flame, *Int J Hydrogen Energy* 41(21): 9219-26.

[15] Joo S, Yoon J, Kim J, Lee M, Yoon Y, 2015. NOx emissions characteristics of the partially premixed combustion of H2/CO/CH4 syngas using artificial neural networks, *Appl Therm Eng* 80: 436 - 44

[16] Zhang Y, Shen W, Zhang H, Wu Y, Lu J, 2015. Effects of inert dilution on the propagation and extinction of lean premixed syngas/air flames, *Fuel* 157: 115-21.

[17] Boivin P, Jiménez C, Sánchez AL, and Williams FA, 2011. A four-step reduced mechanism for syngas combustion, *Combust Flame* 158(6): 1059-63.

[18] Williams TC, Shaddix CR, and Schefer RW, 2007. Effect of Syngas Composition and CO2-Diluted Oxygen on Performance of a Premixed Swirl-Stabilized Combustor*, Combust Sci Technol* 180(1): 64-88.

[19] Azimov U, Tomita E, Kawahara N, and Harada Y, 2011. Effect of syngas composition on combustion and exhaust emission characteristics in a pilot-ignited dual-fuel engine operated in PREMIER combustion mode, *Int J Hydrogen Energy* 36(18): 11985-96.

[20] Lee MC, Seo SB, Chung JH, Kim SM, Joo YJ, and Ahn DH, 2010. Gas turbine combustion performance test of hydrogen and carbon monoxide synthetic gas, *Fuel* 89(7): 1485-91.

[21] Ouimette P and Seers P, 2009. NOx emission characteristics of partially premixed laminar flames of H_2/CO/CO_2 mixtures, *Int J Hydrogen Energy* 34(23): 9603-10.

[22] Watson GMG, Munzar JD, Bergthorson JM, 2014. NO formation in model syngas and biogas blends, *Fuel* 124: 113-124.

[23] Lieuwen T, McDonell V, Petersen E, Santavicca D, 2008. Fuel flexibility influences on premixed combustor blowout, flashback, autoignition, and stability, *J Eng Gas Turbines Power* 130: 011506.

[24] Strakey P, Sidwell T, Ontko J, 2007. Investigation of the effects of hydrogen addition on lean extinction in a swirl stabilized combustor, *Proc Combust Inst* 31(2): 3173-3180.

[25] Schafer RW, Wicksall DM, Agrawal AK, 2002. Combustion of hydrogen-enriched methane in a lean premixed swirl-stabilized burner, *Proc Combust Inst* 29(1): 843-851.

[26] Li S, Zhang X, Zhong D, Weng F, Li S, and Zhu M, 2016. Effects of inert dilution on the lean blowout characteristics of syngas flames, *Int J Hydrogen Energy* 41(21): 9075-86.

[27] Sayad P, Schönborn A, and Klingmann J, 2016. Experimental investigation of the stability limits of premixed syngas-air flames at two moderate swirl numbers, *Combust Flame* 164: 270-82.

[28] García-Armingol T and Ballester J, 2015. Operational issues in premixed combustion of hydrogen-enriched and syngas fuels, *Int J Hydrogen Energy* 40(2): 1229-43.

[29] Shanbhogue SJ, Husain S, Lieuwen T, 2009. Lean blowoff of bluff body stabilized flames: Scaling and dynamics, *Prog Energy Combust Sci* 35(1): 98–120.

[30] Trunk PJ, Boxx I, Heeger C, Meier W, Bohm B, Dreizler A, 2013. Premixed flame propagation in turbulent flow by means of stereoscopic PIV and dual-plane OH-PLIF at sustained kHz repetition rates, *Proc Combust Inst* 34(2): 3565–3572.

[31] Driscoll JF, 2008. Turbulent premixed combustion: Flamelet structure and its effect on turbulent burning velocities, *Prog Energy Combust Sci* 34(1): 91–134.

[32] Valera-Medina A, Syred N, Griffiths AJ, 2009. Visualisation of isothermal large coherent structures in a swirl burner, *Combust Flame* 156(9): 1723–1734.

[33] Litvinov IV, Shtork SI, Kuibin PA, Aleseenko SV, Hanjalic K, 2013. Experimental study and analytical reconstruction of precessing vortex in a tangential swirler, *Int J Heat Fluid Flow* 42: 251–264.

[34] Syred N, Giles A, Lewis JP, Abdulsada MH, Valera-Medina A, Marsh R, Bowen PJ, Griffiths AJ, 2014. Effect of inlet and outlet configurations on blow-off and flashback with premixed combustion for methane and a high hydrogen content fuel in a generic swirl burner, *Appl Energy* 116: 288-296.

[35] Zimont, V, Polifke, W, Bettelini M, Weisenstein W, 1998. An Efficient Computational Model for Premixed Turbulent Combustion at High Reynolds Numbers Based on a Turbulent Flame Speed Closure, *J Gas Turbines Power* 120 (3): 526- 532.

[36] ANSYS Fluent, Shear-Stress Transport (SST) k-ω Model [Online] Available: https://www.sharcnet.ca/Software/Fluent6/html/ug/node487.htm [Accessed 13th April 2017]

[37] O'Doherty T and Lucca- Negro O, 2001. Vortex breakdown: a review. *Prog Energy Combust Sci* 27(4): 431-481.

[38] O'Doherty T, Gardner R, 2005.Turbulent length scales in an Isothermal Swirling Flow, 8th Symposium on Fluid Control, Measurement and Visualization, Chengdu, China.